Molecular Biology Reports (2022) 49:1113–1120
https://doi.org/10.1007/s11033-021-06936-3

ORIGINAL ARTICLE

Antineoplastic effectiveness of silver nanoparticles synthesized from *Onopordum acanthium* L. extract (AgNPs-OAL) toward MDA-MB231 breast cancer cells

Romina Delalat[1] · Seyed Ataollah Sadat Shandiz[1] · Bahareh Pakpour[1]

Received: 18 July 2021 / Accepted: 5 November 2021 / Published online: 24 November 2021

Abstract

Background The present research was done to investigate the anticancer properties of silver nanoparticles (AgNPs) fabricated using bioactive extract of *Onopordum acanthium* L. (AgNPs-OAL) against breast cancer cells MDA_MB231 in vitro.

Methods The determination studies of AgNPs-OAL were confirmed by X-ray diffraction (XRD), field emission scanning electron microscopy (FESEM) analysis. Interestingly, the FESEM image observed the spherical shape of AgNPs-OAL with the range of 1–100 nm.

Results As AgNP-OAL exhibited significant cytotoxicity properties on breast cancer MDA_MB231 cells with IC_{50} values of 66.04 µg/mL, while lowing toxicity toward normal human embryonic kidney 293 (HEK293) cells with IC_{50} values of 101.04 µg/mL was evaluated. Further, up-regulation of apoptotic *Bax* and *CAD* gene expressions were confirmed by quantitative real-time reverse transcription-PCR (qRT-PCR) technique results. Moreover, enhanced cell cycle population (sub-G1), annexin V/PI staining, acridine orange and ethidium bromide (AO/EB) staining, Hoescht 33,258 dye, and generation of reactive oxygen species were observed in AgNP-OAL-treated MDA_MB231 cancer cells.

Conclusions The green-synthesized AgNP-OAL has promising anticancer efficiency that can trigger apoptosis pathways in the MDA_MB231 breast cancer cells.

Keywords Silver nanoparticles · Anticancer · Reactive oxygen species · Apoptosis

Introduction

According to the global cancer burden based on the GLOBOCAN 2020, it was estimated that 19.3 million new cancer cases and almost 10.0 million cancer deaths will happen in 2020. Breast cancer is the most frequently diagnosed cancer, with almost 2.3 million new cases reported to be distinguished in 2020 [1]. Many drugs in chemotherapy suffer from different side effects such as enhancing multi-drug resistance (MDR), poor solubility, and undesirable damage to normal cells, which indicate results of commonly therapeutic intervention strategies [2].

Recently, the development of metal nanoparticles is gaining consideration due to their cancer diagnosis, tumor imaging, and drug delivery [3].

Recently, AgNPs have unique electrical, optical, and thermal characteristics and been reported to display wound healing, antibacterial activities, [4] antimicrobial, [5] antioxidant, [6] and anticancer properties [7]. The fabrication of nanoparticles is mediated through a variety of chemical, physical, and biological strategies [8]. There is an increased interest in the synthesis of nanoparticles using the green fabrication method used by plants owning to their various advantages such as simple, cost effective, environmentally eco-friendly, and not requiring hazardous chemicals [9]. On the other hand, *Onopordum acanthium* L. is a flowering plant belonging to the family Asteraceae, with rich phytochemical compounds. *Onopordum acanthium* L. displayed significant medical activities such as antiradical, antibacterial, antihypertensive, cardiotonic agent, antitumor, and anti-inflammatory activities [10].

✉ Seyed Ataollah Sadat Shandiz
Ata.sadatshandiz@iauctb.ac.ir

[1] Department of Biology, Central Tehran Branch, Islamic Azad University, Tehran, Iran

In this context, we have explored the apoptotic activity of AgNPs using *Onopordum acanthium* L. (AgNPs-OAL) extract as a reducing agent. The FESEM was utilized to identify the morphological feature of the nanoparticles. The crystalline nature of nanoparticles was explored using XRD. The *in vitro* cytotoxicity was performed in MDA-MB231 (human breast cancer), and HEK293 (human embryonic kidney) cell lines upon treatment with prepared AgNPs-OAL. Moreover, cell cycle analysis, morphological properties of apoptotic/necrotic cells, ROS generation, apoptotic *Bax* and *CAD* gene expressions, and induction of apoptosis/necrosis were also evaluated by Annexin V/PI staining to explore the significant impacts of the AgNPs-OAL as anticancer agents.

Materials and methods

Fabrication and determination of green AgNPs-OAL

For preparation of plant extract, the powder form (50 g) of dried plant *Onopordum acanthium* L. was added to 200 cc of solvent ethanol (50%) and centrifuged for 20 min at 14,000 rpm. The resulting extract was filtered through a filter paper and then stored in the refrigerator before. The extract of *Onopordum acanthium* L. about 5 mL was added dropwise in 100 mL 1 mM silver nitrate ($AgNO_3$, 99%) solution with constant stirring at room temperature. To collect the suspension, *Onopordum acanthium* L. extract-derived AgNPs (AgNPs-OAL) were centrifuged at 13,000 rpm for 20 min. The determination studies were confirmed by X-ray diffraction XRD and FESEM analyzes. The crystalline nature of AgNPs-OAL was characterized by XRD (Burker AXS D8 X-Ray diffractometer) instrument using Cu Kα radiation in 2θ range of 5°-80°. The particle morphology of prepared AgNPs-OAL was imaged and analyzed through FESEM (Philips XL30) instrument.

Cell culture

MDA-MB231 (human breast cancer) (C578), HEK293 (C630) (human embryonic kidney) cell lines were procured from NCBI (National Cell Bank of Iran), Pasteur Institute of Iran. The cells were sustained in $RPMI_{1640}$ media pH= 7.2 with 10% Fetal bovine serum FBS (Gibco, U.S). The medium was added with 1% penicillin/streptomycin solution, followed by incubation at 5% CO2, 37 °C.

Viability assay

The percentage of cell viability has been evaluated toward MDA-MB231 and HEK293 cell lines via the MTT method followed by treatment with AgNPs-OAL according to previous standard protocol [11]. All the cells (1×10^4 cell /well) were grown in 96-well plates and exposed to various test doses (0, 0.625, 12.5, 25, 50, and 100 µg/mL) of AgNPs-OAL. After 24 h incubation, MTT solution (5 mg/mL) was introduced into each well for 4 h. The formazan crystals formed followed by adding MTT dye. DMSO solution was added to samples to improve dissolving, followed by recording the absorbance value at 570 nm using an ELISA microplate reader. The data are presented as the mean ± SEM of three replicates from three independent experiments.

Analysis of apoptotic gene expressions

The apoptotic *Bax* and *CAD* gene expressions in AgNPs-OAL-treated cells were distinguished through SYBR Green real-time quantitative PCR at the mRNA level. The cells were firstly treated with AgNPs-OAL in IC_{50} concentration overnight. The RNA-isolation kit was used for the isolation of the total cellular RNA (Qiagen, Valencia, CA) based on manufacturer's protocols. Then, complementary DNA (cDNA) was fabricated in terms of the manufacturer's protocols using a PrimeScript™ RT Kit (Takara, Japan). The primers utilized for RT-PCR were: forward 5′ CGGCAA CTTCAACTGGGG 3′ and reverse 5′ TCCAGCCCAACA GCCG 3′ for *Bax*, forward 5′ TGGCAGAGATCGGAGAGC AT 3′ and reverse 5′ TCCTTCCATCCCTTCAGAGACTT 3′ for *CAD*. Also, the sequence of the forward primer for Glyceraldehyde 3 phosphate Dehydrogenase *(GAPDH)* as a housekeeping gene was 5′ CCCACTCCTCCACCTTTGAC 3′ and that of reverse primer was 5′ CATACCAGGAAATGA GCTTGACAA 3′. The ratio formula ($2^{-\Delta\Delta Ct}$) was used to assess the apoptotic gene expressions.

In vitro apoptosis/necrosis assay

The quantification of the mode of AgNPs-OAL-induced cell death in the MDA-MB231 cells were assessed using flow cytometry followed by staining with fluorescein isothiocyanate (FITC)-Annexin V and propidium iodide (PI) staining in terms of the kit's Protocol (Roch, Switzerland). For this, the cells (3×10^5 cells/well) were subjected to 66.04 µg/mL of AgNPs-OAL, allowed to grow for 24 h. The treated cells were washed by PBS, re-suspended in binding buffer, and staining with PI and Annexin V followed by incubation in the dark. After incubated for 10 min, the percentage of the apoptotic and necrotic cells was ascertained through flow cytometer [12].

2′,7′-Dichloro dihydro fluorescein diacetate (DCFH-DA) assay

Intracellular ROS generation was distinguished using flow cytometry [13]. The cells (MDA-MB231, 3×10^5 cell / well) were seeded in 6-well plates for 24 h followed by the

addition of required concentration of AgNPs-OAL. The MDA-MB231 cells were washed with phosphate-buffered saline and then cells were exposed with DCFH-DA dye after a further treatment of 30 min. The stained cells were further investigated via flow cytometer for determination of ROS production.

Cell cycle analysis

Flow cytometric analysis was determined to investigate the changes in cell cycle evaluation in AgNPs-OAL treated MDA-MB231 cells. The MDA-MB231 cells were cultured in 6-well plates and exposed with 66.04 (µg/mL) of the AgNPs-OAL in the CO_2 incubator for 24 h.

Further, the cells were harvested and washed with PBS. After fixation in ice 70% ethanol, the cells were then stained with PI, followed by treatment of RNase A (100 µg/ml). Finally, the DNA content of stained cells was measured through a flow cytometer.

Morphology of apoptotic/necrotic cells

Determination of apoptotic/necrotic cells was investigated by a dual acridine orange and ethidium bromide (AO/EB) and Hoechst nuclear staining. The MDA-MB231 cells were treated with 66.04 µg/mL of AgNPs-OAL. After washing with PBS, control and treated cells were fixed with 4% formaldehyde and stained with 10 µL of AO/EB solution for 5 min incubation.

For the Hoechst 33,258 staining, MDA-MB231 cells were subjected to six-well plating, overnight incubation with AgNPs-OAL, staining with Hoechst 33,258 solutions for 5 min in the dark, followed by washing thrice with PBS. For observation, treated and control cells were visualized for their apoptotic to the nuclei using fluorescence microscopy images.

Result and discussion

Characterization of AgNPs-OAL

In recent decades, AgNPs fabricated using biological methods has a promising impact on cancer cell lines [14, 15]. Plant mediated green strategy for AgNPs synthesis can be superior to fungal and bacterial-mediated strategies because of their accessibility, environmentally friendly procedures, and safety methods [16–18]. In this investigation, *Onopordum acanthium* L. extract was used to fabricate AgNPs. As the *Onopordum acanthium* L. extract was mixed with silver nitrate solution, the color variation was seen in the solution that converted into the dark brown overnight, indicating the fabrication of silver nanoparticles by phytoconstituents of *Onopordum acanthium* L. extract.

XRD pattern of particles confirms the crystallinity level of the AgNPs-OAL' structure (Fig. S1). Intense peaks of silver nanoparticles from the extract of *Onopordum acanthium* L. were visualized at 37.93°, 43.88°, 64.13° and 77.13° in the 2θ range noted at (111), (200), (220) and (311) diffraction pattern, respectively. The reflection planes of the fabricated AgNPs-OAL were consistent with earlier investigations [12, 19]. The FESEM analysis was investigated to find out the shapes and morphology of the produced AgNPs-OAL. The AgNPs-OAL was spherically shaped with a size in the range of 1–100 nm (Fig. 1).

Cytotoxicity effect of AgNPs-OAL on MDA-MB-231cells

In this study, cytotoxicity of AgNPs-OAL was examined toward MDA-MB-231 and HEK293 cells at a concentration of 6.25 to 100 µg/mL using MTT assay. In studies conducted by other groups, it was reported that that HEK293 cells as a normal (non cancerous cells). These cells were initially thought to originate from an endothelial, epithelial, or fibroblastic cell from the fetal kidney and frequently used as non- or low tumorigenic for testing oncogenic properties of cancer-associated genes [20, 21].

According to some articles and performing MTT test with different doses, selected doses such as: 0, 0.625, 12.5, 25, 50, and 100 µg/mL have been the most appropriate doses to compare the effect of AgNPs-OAL on cancer cell lines. Different types of reports are available on anti-tumor effect of green silver nanoparticles toward various cell lines such as AGS [22], MCF-7 [23], and human prostate cancer LNCaP cells [24]. Al Tamimi et al. in their study exhibited the fabrication of Silver–copper alloy nanoparticles (AgCu-NP), Cu-NP, and Ag-NP, and showed that AgCu-NP increased

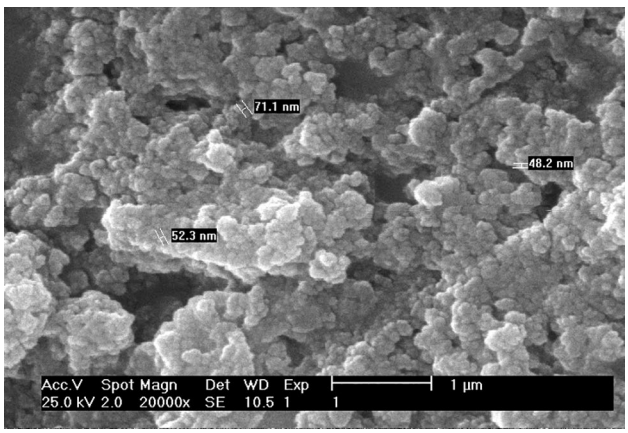

Fig. 1 FESEM image of the silver nanoparticles fabricated using bioactive extract of *Onopordum acanthium* L

toxicity against MCF-7 breast cancer cells at 10 µg/mL concentration, while as AgNPs and CuNPs have no significant toxic effect [25]. The silver nanoparticles fabricated by black tea leaf inhibited the cell viability of He-La cervical cancer cell lines up to 75% [26]. Moreover, AgNP were shown to inhibit the angiogenesis, metastasis and induce apoptosis in HER2 Positive Breast cancer cells [27]. Interestingly, AgNPs-OAL showed significant dose-dependency on cell viability followed by increased concentrations. The IC_{50} values of AgNPs-OAL against MDA-MB231 and HEK293 cells were 66.04 and 101.04 µg/mL, respectively. The in vitro cell viability was exhibited as 85% in AgNPs-OAL at 12.5 µg/mL; however, the viability percentage was remarkably reduced to 45% at 100 µg/mL of nanoparticles (Fig. S2). Herein, we showed that MDA-MB-231 cells are more sensitive to AgNPs-OAL than normal HEK293 cells. Different doses of nanoparticles were reported in other studies.

Our results are consistent with the results of [28], where biologically synthesized AgNPs using *Bacillus funiculus* culture supernatant, it recorded significant cytotoxicity against MDA-MB-231 cell line in a dose dependent manner, with IC_{50} value of 8.7 µg/mL [28]. Also, Ghandehari et al. (2019) reported apoptotic properties of *Rubia tinctorum* produced AgNPs toward the MDA-MB-231 cell line (IC_{50}=4 µg/mL/48 h). These findings imply that fabricated AgNPs-OAL depressed MDA-MB-231 cell viability [29]. According to our MTT results, AgNPs-OAL exhibited dose-dependent relationship on the viability of MDA-MB-231cells, which could be related to the synergetic activities of functional groups derived from *Onopordum acanthium* L. attaching to the AgNPs. Moreover, the impacts of green-fabricated AgNPs in MDA-MB-231 are consistent with earlier studies [30, 31].

Measurement of ROS production

The ROS are produced in normal cells and have roles in many physiological conditions [32]. Under excessiveness of ROS, a series of cellular events were occurring which resulted in lipid peroxidation, DNA damaging, cell cycle arrest, and promote apoptosis pathway [33]. It has been reported that new strategies for targeting ROS contribute to cancer therapy [13]. Various reports have elucidated the roles of different nanometals in triggering ROS content in different cancer cells [34, 35]. Zhu et al. reported that AgNPs could induce human hepatocellular carcinoma HepG-2 cell apoptosis via ROS-mediated MAPKs, AKT, and p53 signaling pathways [36]. Moreover, ROS production in cancers modulates the different signaling pathways by regulating apoptosis, angiogenesis, and proliferation [37].

In our study, ROS production in treated MDA-MB231 cells was 71.7%, while the control cells were 4.08%. In this study, the ROS production in MDA-MB231 cells was illustrated in Fig. 2. Maximum production of ROS was closely exhibited for AgNPs-OAL, resulting in high cytotoxicity on MDA-MB231 cells as presented in the above results.

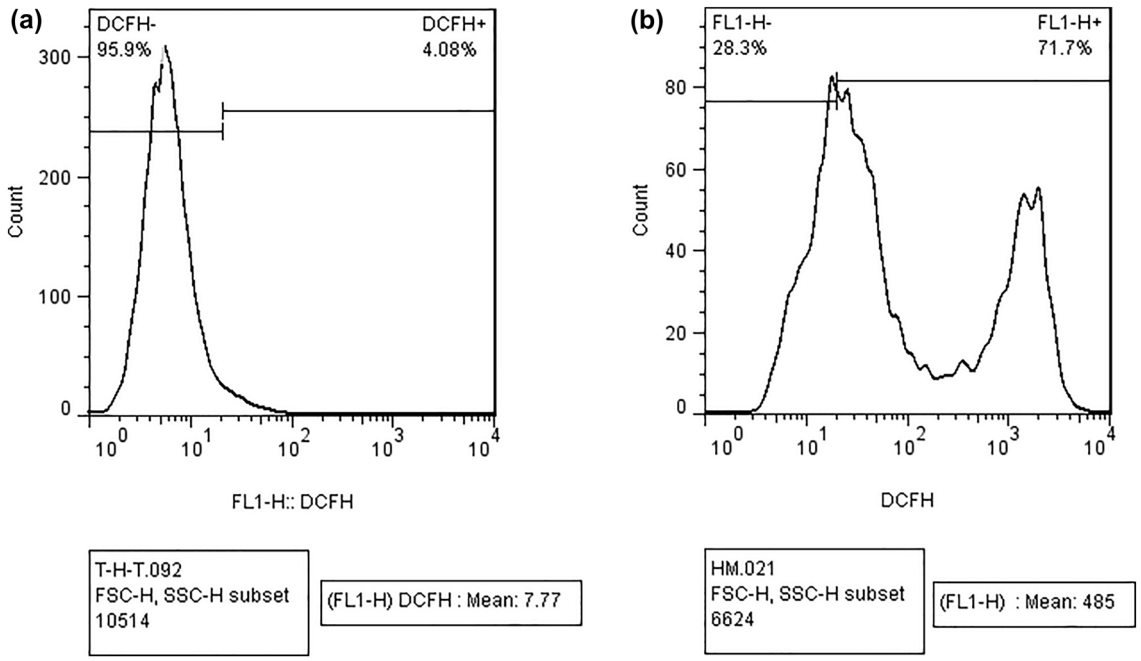

Fig. 2 Effect of the produced AgNPs-OAL on ROS generation in untreated (**a**) and treated (**b**) MDA_MB231 cells utilizing DCFH-DA followed by flow cytometry

AgNPs-OAL induce apoptosis in MDA-MB231 cells

Apoptosis represents a well-defined intracellular physiological cell death that often doesn't trigger the inflammatory response [38]. Effector caspase 3 activations are required for efficient execution of apoptotic death [39]. Translocation and cleavage of caspase-activated DNAse (CAD) were activated by caspase 3, results in DNA fragmentation.

In the current study, we evaluated the roles of pro-apoptotic *Bax* and *CAD* regulation concerning to the apoptotic death of cancer cells [33]. The mRNA expression levels of genes in AgNPs-OAL—mediated apoptotic cells were displayed by the qRT-PCR method, presented in Fig. S3. The expression of the *CAD* and pro-apoptotic *Bax* genes was enhanced by a 4.04-fold, and 1.38 fold in AgNPs-OAL treated MDA-MB231 cells, respectively.

Annexin V/PI staining determined the MDA-MB231 cells undergoing programmed cell death and necrosis (Fig. 3). We found that the AgNPs-OAL enhanced the number of early and late apoptosis on MDA-MB231 by 47.8% at 66.04 µg/mL. In the report conducted by Mohammadi-Ziveh et al., the apoptotic property of Ag-S.Khuzistanica on the colorectal HT29 cancer cell line was investigated. They indicated that 375, 750, 1500, 3000 µg/mL of Ag- *S.Khuzistanica* could increase the apoptosis rate (~ 30%) along with the up-regulation of apoptotic index ratio. In our study, the apoptosis rate (47.8%) was much higher after exposure to AgNPs-OAL than the Mohammadi-Ziveh results (~ 30%) [40].

According to the main pattern of nanoparticles in apoptosis, the cell cycle results were conducted on AgNPs-OAL -exposed MDA-MB231 cells. The cellular DNA of treated MDA-MB231 cells was stained with PI, followed by testing the DNA content via flow cytometry assay. Herein, the proportion of AgNPs-OAL-exposed cells in the apoptotic cell population (sub-G1) phase was increased from 7.04 to 12.58% in MDA-MB231 cells (Fig. 4). A comparison of the Annexin V/PI staining and cell cycle results indicates that the exposure of MDA-MB231 cells with AgNPs-OAL cause inhibition of the sub-G1 phase and the up-regulation of apoptosis by increasing the early and late phase of the apoptosis pathway.

Moreover, we employed a further examination to determine the possible stimulation role of AgNPs-OAL in the apoptosis pathway. Given that the previous section demonstrated that the AgNPs-OAL can trigger an apoptosis pathway, the alterations in the nuclear morphology of apoptotic, necrotic cells were tested by AO/EB double staining and Hoescht 33,258 after treated with AgNPs-OAL.

The Hoescht 33,258 results show AgNPs-OAL-treated cells have enhanced apoptosis via cell structure abnormality, bright color, and condensed chromatin (Fig. 5).

At the concentration of 66.04 µg/mL, AO/EB double staining was investigated to discriminate the variations in apoptotic and normal cells. The Fig. 6 shows that treated cells display apoptosis by changing the color of the nucleus into orange, while green nuclei represent untreated cells. Nanoparticles-exposed MDA-MB231 cells demonstrated an increase in the cell shrinkage and nuclear fragmentation compared to untreated cells, exhibiting the promotion of apoptosis pathway by the fabricated AgNPs-OAL. Thus, the results exhibited that the AgNPs-OAL increased cell death, leading to the induction of apoptosis pathway.

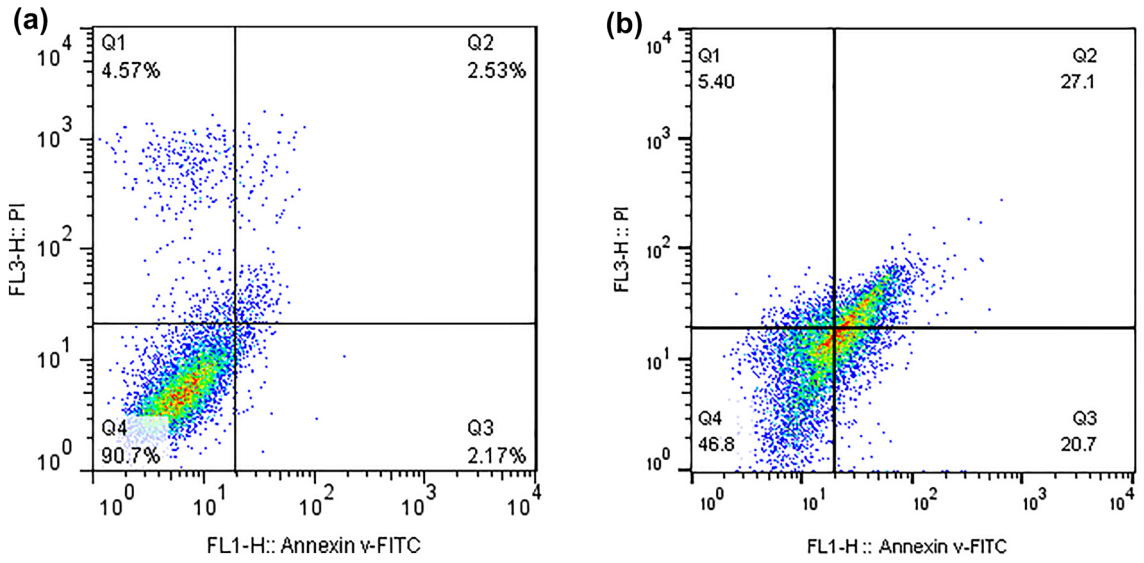

Fig. 3 Evaluation of apoptosis/necrosis in MDA-MB231 cancer cells by flow cytometric analysis. **a** Negative control **b** Annexin/PI staining of exposed cells to AgNPs-OAL at 66.04 µg/mL

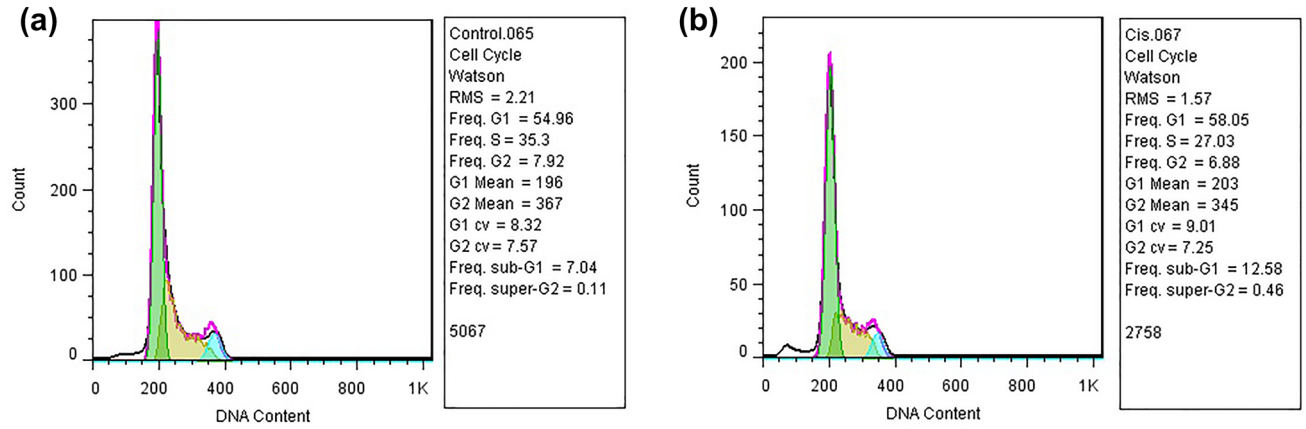

Fig. 4 Effect of AgNPs-OAL after 24 h treatment on cell cycle arrest analysis of **a** untreated and **b** treated MDA-MB231 cells

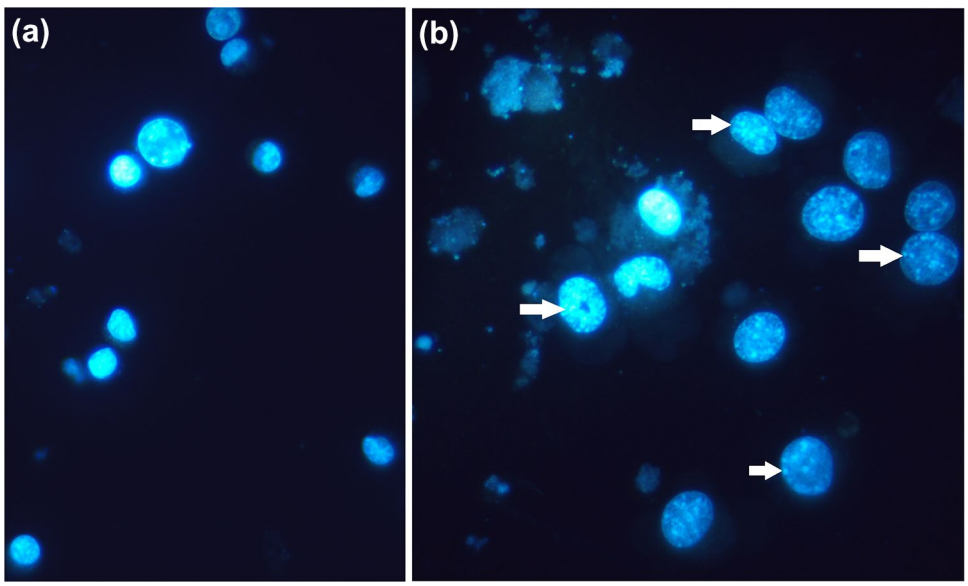

Fig. 5 Morphology properties of MDA_MB231 cells with Hoescht 33,258 staining under fluorescence microscope, **a** untreatment as control **b** the cells exposed to IC_{50} of synthetic AgNPs-OAL for 24 h. The arrow revealed the apoptotic cells

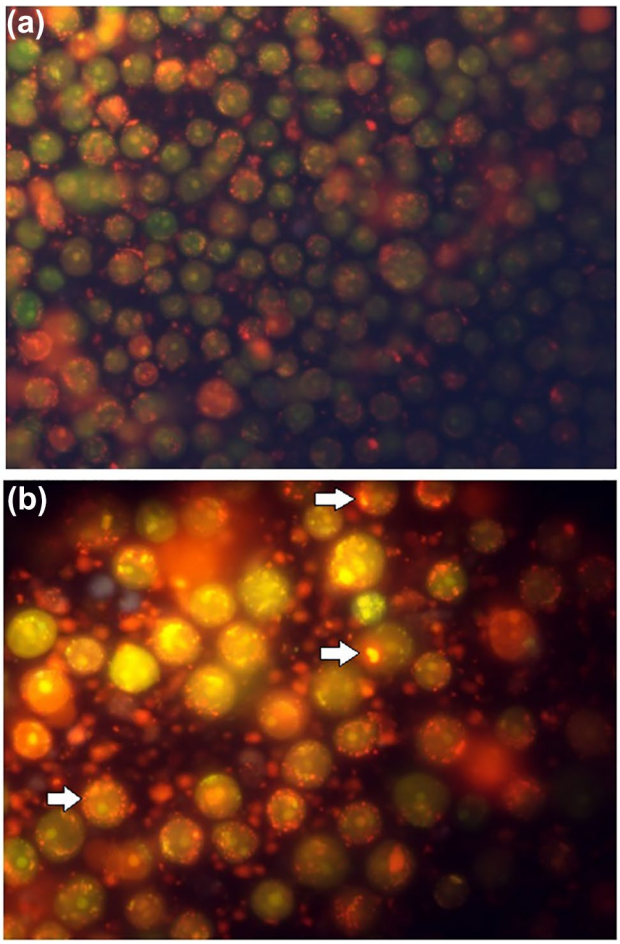

Fig. 6 Morphology changes of **a** untreated and **b** treated MDA_MB231 cells with fabricated AgNPs-OAL following AO/EB dye under fluorescence microscope. The arrow revealed the apoptotic cells

Conclusions

In summary, plant-mediated AgNPs synthesis from *Onopordum acanthium* L. extract was generated by the green fabrication route. Determinations of the obtained nanoparticles were conducted by FESEM and XRD analysis. The in vitro cytotoxicity assay results, apoptotic genes expressions, cell cycle analysis, annexin V/PI staining, AO/EB staining, Hoescht 33,258 staining, and generation of ROS exhibited that fabricated AgNPs could act as a promising strategy in the treatment of breast cancer in the future.

Supplementary Information The online version contains supplementary material available at https://doi.org/10.1007/s11033-021-06936-3.

Author contributions Conceptualization: SASS and RD, Methodology: SASS, Formal analysis: RD, Investigation: RD, Resources: AS, Data curation: SASS and BP, Writing—original draft preparation: SASS, Visualization: SASS and BP supervision, SASS.

Declarations

Conflict of interest The authors declare no conflict of interest.

References

1. Sung H, Ferlay J, Siegel RL, Laversanne M, Soerjomataram I, Jemal A, Bray F (2021) Global cancer statistics 2020: GLOBOCAN estimates of incidence and mortality worldwide for 36 cancers in 185 countries. CA A Cancer J Clin 71(3):209–249
2. Acharya D, Satapathy S, Somu P, Kumar Parida U, Mishra G (2020) Apoptotic effect and anticancer activity of biosynthesized silver nanoparticles from marine algae *Chaetomorpha linum* extract against human colon cancer cell HCT-116. Biol Trace Elem Res 199(5):1812–1822
3. Kumari R, Saini AK, Kumar A, Saini RV (2019) Apoptosis induction in lung and prostate cancer cells through silver nanoparticles synthesized from *Pinus roxburghii* bioactive fraction. JBIC J Biol Inorg Chem 25:23–37
4. Riaz M, Mutreja V, Sareen S et al (2021) Exceptional antibacterial and cytotoxic potency of monodisperse greener AgNPs prepared under optimized pH and temperature. Sci Rep 11:2866. https://doi.org/10.1038/s41598-021-82555-z
5. Soliman H, Elsayed A, Dyaa A (2018) Antimicrobial activity of silver nanoparticles biosynthesised by Rhodotorula sp. strain ATL72. Egyptian J Basic Appl Sci 5(3):228–233
6. Salari S, Esmaeilzadeh Bahabadi S, Samzadeh-Kermani A, Yosefzaei F (2019) In-vitro evaluation of antioxidant and antibacterial potential of green synthesized silver nanoparticles using *Prosopis farcta* fruit extract. Iran J Pharm Res 18(1):430–455
7. Venugopal K, ARather H, Rajagopal K, Shanthi MP, Sheriff K, Illiyas M et al (2017) Synthesis of silver nanoparticles (Ag NPs) for anticancer activities (MCF 7 breast and A549 lung cell lines) of the crude extract of *Syzygium aromaticum*. J Photochem Photobiol B Biol 167:282–289
8. Almalki MA, Khalifa AYZ (2020) Silver nanoparticles synthesis from Bacillus sp KFU36 and its anticancer effect in breast cancer MCF-7 cells via induction of apoptotic mechanism. J Photochem Photobiol B Biol 204:111786
9. Kiran P, Shejawal DS, Randive SD, Bhinge MA, Bhutkar, Sachin S, Todkar AS, Mulla, Namdeo R, Jadhav (2021) Green synthesis of silver, iron and gold nanoparticles of lycopene extracted from tomato: their characterization and cytotoxicity against COLO320DM, HT29 and Hella cell. J Mater Sci. https://doi.org/10.1007/s10856-021-06489-8.
10. Garsiya ER, Konovalov DA, Shamilov AA, Glushko MP, Orynbasarova KK (2019) A traditional medicine plant, *Onopordum acanthium* L. (Asteraceae): chemical composition and pharmacol research. Plants (Basel) 8(2):40
11. Hira I, Kumar A, Kumari R, Saini AK, Saini RV (2018) Pectinguar gum-zinc oxide nanocomposite enhances human lymphocytes cytotoxicity towards lung and breast carcinomas. Mater Sci Eng C 90:494–503
12. Prakash P, Gnanaprakasam P, Emmanuel R, Arokiyaraj S, Saravanan M (2013) Green synthesis of silver nanoparticles from leaf extract of *Mimusops elengi*, Linn. for enhanced antibacterial activity against multi drug resistant clinical isolates. Colloids Surf B Biointerfaces 108:255–259
13. Mitra S, Nguyen LN, Akter M, Park G, Choi EH, Kaushik NK (2019) Impact of ROS generated by chemical, physical, and plasma techniques on cancer attenuation. Cancers 11(7):1030–1061

14. Shameli K, Bin Ahmad M, Jaffar Al-Mulla EA, Ibrahim NA, Shabanzadeh P, Rustaiyan A, Abdollahi Y, Bagheri S, Abdolmohammadi S, Usman MS, Zidan M (2012) Green biosynthesis of silver nanoparticles using *Callicarpa maingayi* stem bark extraction. Molecules 16(7):8506–8517**17**
15. Haider AJ, Mohammed MR, Al-Mulla EAJ et al (2014) Synthesis of silver nanoparticle decorated carbon nanotubes and its antimicrobial activity against growth of bacteria. Rend Fis Acc Lincei 25:403–407. https://doi.org/10.1007/s12210-014-0300-6.
16. Ratan ZA, Haidere MF, Nurunnabi M, Shahriar SM, Ahammad A, Shim YY et al (2020) Green chemistry synthesis of silver nanoparticles and their potential anticancer effects. Cancers 12(4):855. https://doi.org/10.3390/cancers12040855
17. Wang T, Yang L, Zhang B, Liu J (2010) Extracellular biosynthesis and transformation of selenium nanoparticles and application in H_2O_2 biosensor. Colloids Surf B 80(1):94–102
18. Chen H, Yoo JB, Liu Y, Zhao G (2011) Green synthesis and characterization of selenium nanoparticles and nanorods. Electron Mater Lett 7:333–336
19. Das J, Das MP, Velusamy P (2013) *Sesbania grandiflora* leaf extract mediated green synthesis of antibacterial silver nanoparticles against selected human pathogens. Spectrochim Acta Part A 104:265–270
20. Dumont J, Euwart D, Mei B, Estes S, Kshirsagar (2016) Human cell lines for biopharmaceutical manufacturing: history, status, and future perspectives. Crit Rev Biotechnol 36(6):1110–1122
21. Wahab R, Kaushik N, Khan F et al (2016) Self-styled ZnO nanostructures promotes the cancer cell damage and supresses the epithelial phenotype of glioblastoma. Sci Rep 6:19950. https://doi.org/10.1038/srep19950.
22. Mousavi B, Tafvizi F, Bostanabad SZ (2018) Green synthesis of silver nanoparticles using *Artemisia turcomanica* leaf extract and the study of anti-cancer effect and apoptosis induction on gastric cancer cell line (AGS). Artifi Cells Nanomed Biotech 46(1):499–510
23. Devaraj P, Kumari P, Aarti C, Renganathan A (2013) Synthesis and characterization of silver nanoparticles using cannonball leaves and their cytotoxic activity against MCF-7 Cell Line. J Nanotechnol. 2013:1–5
24. Zhang K, Liu X, Samson OASR, Ramachandran AK, Ibrahim IAA, Nassir AM, Yao J (2019) Synthesis of silver nanoparticles (AgNPs) from leaf extract of Salvia miltiorrhiza and its anticancer potential in human prostate cancer LNCaP cell lines. Art Cells Nanomed Biotechnol 47(1):2846–2854
25. Al Tamimi S, Ashraf S, Abdulrehman T et al (2020) Synthesis and analysis of silver–copper alloy nanoparticles of different ratios manifest anticancer activity in breast cancer cells. Cancer Nano 11:13. https://doi.org/10.1186/s12645-020-00069-1
26. Rajawat S, Malik MM (2019) Anticancer activity of green silver nanoparticles against He-La cervical cancer cell lines. Mater Today Proc 18(3):841–847
27. Vallinayagam S, Rajendran K, Sekar V (2021) Green synthesis and characterization of silver nanoparticles using *Naringi crenulate* leaf extract: key challenges for anticancer activities. J Mol Struct 1243(5):130829
28. Gurunathan S, Woong Han J, Eppakayala V, Jeyaraj M, Kim JH (2013) Cytotoxicity of biologically synthesized silver nanoparticles in MDA-MB-231 human breast cancer cells. Biomed Res Int 2013:535796. https://doi.org/10.1155/2013/535796
29. Ghandehari S, Homayouni Tabrizi M, Ardalan P, Neamati A, Shali R (2019) Green synthesis of silver nanoparticles using Rubia tinctorum extract and evaluation the anti-cancer properties in vitro. IET Nanobiotechnol 13(3):269–274
30. Bandyopadhyay A, Roy B, Shaw P et al (2020) Cytotoxic effect of green synthesized silver nanoparticles in MCF7 and MDA-MB-231 human breast cancer cells in vitro. Nucleus 63(2):191–202
31. Juarez-Moreno K, Gonzalez EB, Girón-Vazquez N, Chávez-Santoscoy RA, Mota-Morales JD, Perez-Mozqueda LL et al (2017) Comparison of cytotoxicity and genotoxicity effects of silver nanoparticles on human cervix and breast cancer cell lines. Hum Exp Toxicol 36(9):931–948
32. Phaniendra A, Jestadi DB, Periyasamy L (2015) Free radicals: properties, sources, targets, and their implication in various diseases. Indian J Clin Biochem 30(1):11–26
33. Ullah I, Talha Khalil A, Ali M, Iqbal J, Ali W, Alarifi S et al (2020) Green-synthesized silver nanoparticles induced apoptotic cell death in MCF-7 breast cancer cells by generating reactive oxygen species and activating caspase 3 and 9 enzyme activities. Oxid Med Cell Longev 2020(4):1215395. https://doi.org/10.1155/2020/1215395
34. Nourmohammadi E, Sarkarizi HK, Nedaeinia R et al (2019) Evaluation of anticancer effects of cerium oxide nanoparticles on mouse fibrosarcoma cell line. J Cell Physiol 234(4):4987–4996
35. Khan BF, Hamidullah, Dwivedi S, Konwar R, Zubair S, Owais M (2019) Potential of bacterial culture media in biofabrication of metal nanoparticles and the therapeutic potential of the as-synthesized nanoparticles in conjunction with artemisinin against MDA-MB-231 breast cancer cells. J Cell Physiol 234(5):6951–6964
36. Zhu B, Li Y, Lin Z et al (2016) Silver nanoparticles induce HePG-2 cells apoptosis through ROS-mediated signaling pathways. Nanoscale Res Lett 11:198. doi:https://doi.org/10.1186/s11671-016-1419-4
37. NavaneethaKrishnan S, Rosales JL, Lee KY (2019) ROS-mediated cancer cell killing through dietary phytochemicals. Oxid Med Cell Longev 2019: 9051542. https://doi.org/10.1155/2019/9051542
38. Rock KL, Kono H (2008) The inflammatory response to cell death. Annu Rev Pathol 3:99–126. https://doi.org/10.1146/annurev.pathmechdis.3.121806.151456
39. Brentnall M, Rodriguez-Menocal L, De Guevara RL et al (2013) Caspase-9, caspase-3 and caspase-7 have distinct roles during intrinsic apoptosis. BMC Cell Biol 14:32. https://doi.org/10.1186/1471-2121-14-32
40. Mohammadi-Ziveh Z, Mirhosseini SA, Mahmoodzadeh Hosseini H (2020) *Satureja khuzestanica* mediated synthesis of silver nanoparticles and its evaluation of antineoplastic activity to combat colorectal cancer cell line. Iran J Pharm Res 19(4):169–180